



CHARACTERIZATION OF FRENCH ACCELEROMETRIC PERMANENT NETWORK STATIONS WITH SURFACE-WAVE BASED METHODS: IMPORTANCE OF JOINT USE OF ACTIVE AND PASSIVE METHODS, LOVE AND RAYLEIGH WAVES

F. Hollender⁽¹⁾, C. Cornou⁽²⁾, A. Dechamp⁽³⁾, F. Renalier⁽⁴⁾, S. Thomassin⁽⁵⁾ and P.-Y. Bard⁽⁶⁾

⁽¹⁾ PhD, CEA, DEN, F-13108 St Paul lez Durance, France, fabrice.hollender@cea.fr

⁽²⁾ PhD, University of Grenoble Alpes /IRD, F-38041 Grenoble, France, cecile.cornou@ujf-grenoble.fr

⁽³⁾ Engineer, CEA, DAM, DIF, 91297 Arpajon, France, aline.dechamp@cea.fr

⁽⁴⁾ PhD, GeophyConsult, 159, quai des Allobroges, F-73000 Chambéry, France, florence.renalier@geophyconsult.com

⁽⁵⁾ PhD, Résonance Ingénieurs-Conseils SA, 1227 Carouge, Switzerland, sylvette.thomassin@resonance.ch

⁽⁶⁾ Scientist, ISTERre, University of Grenoble Alpes / IFSTTAR, F-38058 Grenoble, France, pierre-yves.bard@univ-grenoble-alpes.fr

Abstract

Data provided by accelerometric networks are important for seismic hazard assessment. They are key to derive Ground Motion Prediction Equations (GMPEs). The correct use of accelerometric signal is also linked to the station site metadata that include reliable information about site class (VS30), velocity profiles, and other relevant information that can help to quantify the site effect associated to stations. In France, the permanent accelerometric network consists of about 150 stations. A recent project led to the characterization of around 30 stations, especially in South East of France.

This characterization project was performed using surface-wave based methods that allow the derivation of velocity profiles from dispersion curves of Rayleigh and Love waves. We implemented both active acquisitions (Multichannel Analysis of Surface Waves) along lines from 50 to 100 m length and passive acquisitions (Ambient Vibration Array) using multiple circle arrays (apertures from 10 to 1000 m).

The computation of dispersion curves, then their inversion in terms of shear wave velocity profiles (taking into account the non-uniqueness issue of such inversion) allowed the estimations of VS30 values and the designation of soil classes including the corresponding uncertainties.

From a methodological point of view, this survey leads to the following recommendations: (1) Perform both active and passive measurements in order to derive dispersion curves for an adequate frequency range; (2) perform active acquisitions for both vertical (Rayleigh wave) and horizontal (Love wave) polarities, which reduces the risk of misattribution of modes and thus, mitigates errors when modeling velocity profiles.

Even when logistical contexts are sometimes difficult, the use of surface-wave based methods are suitable for station site characterizations, even on rock sites (where the applicability of these methods was sometimes disputed). Typically, it is possible to achieve a complete survey for one station in one working day, by 5 to 6 motivated operators. Conversely, the processing is time consuming (one working week for one geophysicist) and the inversion procedure has to be supervised by an expert in surface wave methods.

Keywords: Accelerometric network, surface wave methods, velocity profile, Vs30

1. Introduction

Data provided by accelerometric network are important for seismic hazard assessment. They are especially used to derive Ground Motion Prediction Equations (GMPEs). The correct use of accelerometric signal is closely linked to the station site metadata that should provide reliable information about site class, V_{s30} value, velocity profiles, and all relevant information that can help to quantify the site effect associated to stations.

In France, the permanent accelerometric network (“RAP” for “Réseau Accélérométrique Permanent”) consists of approximately 150 stations. We present here a recent effort that led to the characterization of 33 stations, in the South part of France. These stations are briefly presented in section 2. This characterization was performed using surface-wave based methods that allow deriving velocity profiles from dispersion curves of Rayleigh and Love waves. Even if the capabilities of these methods were controversial, when they are implemented with care, they provided good results, as demonstrated within the InterPacific project (e.g. [1-2]). We implemented both active acquisitions (Multichannel Analysis of Surface Waves) and passive acquisitions (Ambient Vibration Array) using multiple circle arrays. The standard acquisition setup is described in section 3 whereas section 4 presents in details the applied processing, taking one station as an example. The computation of dispersion curves, then the inversion in terms of shear wave velocity profiles (taking into account the non-uniqueness issue of such inversion) allowed also defining V_{s30} values and soil class with corresponding uncertainties. Section 5 summarized the results and comments the differences with respect to previous studies. It is worth noting that even for so called "rock sites" ($V_{s30} > 800$ m/s), we almost ever identified a very shallow weathered zone that may be responsible for a high frequency site effect. This one has to be taken into account for a better phenomenological understanding of "high frequency content" of rock station accelerograms (see section 6). From a methodological point of view (section 7), this survey leads to the following recommendations. 1) Perform both active and passive measurements in order to derive dispersion curves on a wide frequency range. 2) Perform active acquisitions for both vertical (Rayleigh wave) and horizontal (Love wave) polarities. This helps to better determine dispersion curve modes and thus decreases the risk of errors in velocity profile derivation.

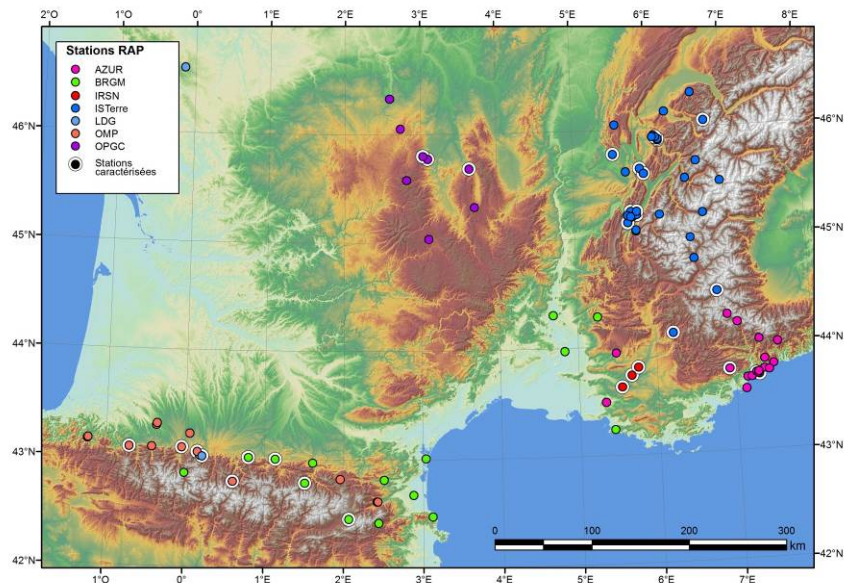


Fig. 1 – Map of the south half of France with location of RAP network stations and stations that benefited of the characterization presented in this paper.

2. Choice of RAP stations

The choice of stations was a compromise between different parameters. We wanted to characterize stations that were used as “reference stations” within the previous work of Drouet *et al.* 2010([3]). We also wanted to characterize stations that produced a high amount of accelerograms. 9 stations were chosen in the Pyrenees area, 3 in Auvergne, 6 in the South part of Alps (Provence and “Cote d’Azur”), 15 in Alps. Figure 1 shows the location of these stations within the whole RAP network. The first surveys were organized in 2012, the last ones finished in January 2015. The processing of 22 surveys is presented here.

3. Overall survey layout and acquisition

The basic acquisition layout consists in the acquisition of both passive (AVA: Ambient Vibration Array) and active (MASW: Multi Analysis Surface waves) surface-wave acquisition. The standard layout was this one:

For MASW acquisition, we used a 24 channel device with 4.5 Hz geophones placed along a line of 46 m, with a geophone inter-trace of 2 m. We strike the ground with a 4 kg hammer on both side of the line (Figure 2). We performed the acquisition with both vertical polarization (for Rayleigh wave analysis) and horizontal polarization (for Love wave analysis). For AVA acquisition, we usually used circle geometries with one sensor in the center and 7 equally-spaced sensors on the circumference of a given radius circle. Acquisitions were made with 15 broad-band seismometers. This number of sensors allowed recording two circular arrays at once (Figure 3). A radius ratio of 3 was chosen to increase two consecutive array radii, starting from a 5 m radius circle up to a 405 m radius circle. For consecutive acquisitions, only the inner/smaller circle was moved to the next larger diameter. Hence, the different sets of acquisitions are:

- Array #1 (called “R1-R2”): center + 5 m and 15 m radius circles,
- Array #2 (called “R2-R3”): center + 15 m and 45 m radius circles,
- Array #3 (called “R3-R4”): center + 45 m and 135 m radius circles,
- Array #4 (called “R4-R5”): center + 105 m and 405 m radius circles.

Of course, this standard layout was adapted to take into account logistical constraints. For the Pyrenees and Auvergne stations surveys, performed in 2012, we just had 10 sensors and we use single circle geometries. For (a priori) rock sites, we usually skip Array #1 (due to lack of energy at high frequency and high velocity) and we instead performed two MASW lines (the standard one with its 46 m line and 2 m spaced geophones and a second one with a 92 m line and 4 m spaced geophones). For sites with very difficult access, we also sometimes skip Array #4.

From a theoretical point of view, AVA survey has to be performed on a flat surface. On a few sites (OGLE, OGMU, GRN, OGS) only MASW measurements were performed because topography did not allow performing AVA. For all other sites that produced a successful AVA processing, all sensors could be assumed to be located in a flat plane (not necessary horizontal) with sometimes a moderate distance to this plane (+/- 15%).



Figure 2 – Left: MASW line near the CALF station. Right: MASW acquisition (4 kg hammer source) near the OGCH station.



Figure 3 – Left: location of the 15 broadband seismometers on a double circle geometry (here, with radii of 15 and 45 m) at the OGAP station. Right: inner circle (radius = 5 m) of an AVA acquisition near the OGAP station.

4. Example of a complete processing: the OGIM station

Overall geological context:

The OGIM site is located in the north-east of Grenoble in the clayey cone of Saint-Ismier (end Würmien – Holocene). It is surrounded by torrential cones interstratified in recent alluvial deposits (Holocene to current). Marious deposits (middle and higher Jurassic) outcrop to the south-west of the site. At the scale of the acquisition, the topography is flat, consisting in a plane gently dipping to the south east. All sensors could be assumed to be placed on the same plane.

Processing results:

All processing was performed with the Geopsy software package (Wathelet 2008 [4]).

In order to check the overall quality of data, we computed Fourier amplitude, and then the ambient vibration H/V curves (Figure 4). The H/V analysis can provide the fundamental frequency of the site (that could be include later within the inversion) and give information about the possible lateral heterogeneity, especially for large array.

On AVA arrays, we systematically applied FK processing, high resolution FK (HRFK) processing and MSPAC processing. The results are shown Figure 5. Then the dispersion curves (DCs) associated to each geometry / processing type were picked (when possible), with respect to the wave-number validity range. In our example, MSPAC did not produce clear information for Array R4R5. For MASW (Figure 6), both vertical (Rayleigh) and horizontal (Love) polarization were processed, for each shot position, then the “beampower” was picked, also respecting validity range criteria.

Then, the different DCs curves are gathered (Figure 7). When FK (or HRFK) and MSPAC produced different DCs, we checked the back-azimuth of dominant vibrations. Indeed, MSPAC approach assumes that the vibration sources are homogeneously distributed in azimuth. When this assumption is not respected, we avoided to use MSPAC results.

The inversions were performed with the inversion tool of the Geopsy software package, which uses a global search approach with a neighborhood algorithm ([4]). The broad-band dispersion curves previously derived were inverted, which in most cases involved joint inversion of both the Rayleigh and Love dispersions curves, with sometimes several different modes. For sites where a clear fundamental frequency could also be deduced from the H/V analysis, and when the dispersion curve at the lowest frequency was close to f_0 , the f_0 value was also used in a joint inversion. In the OGIM case, inversion results were obtained after 300300 models. Figure 8 displays the best shear-wave velocity profile (red line) as well as the ensemble of shear-wave velocity profiles that explain the data within their uncertainty bound following the “acceptable solution” concept. Theoretical dispersion curves obtained from this ensemble of ground models are also shown together with the observed phase velocities.

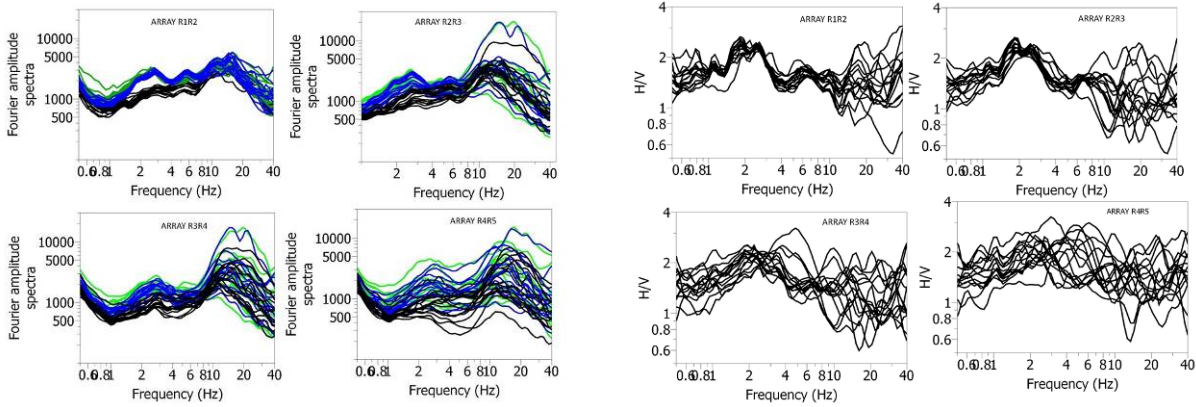


Figure 4 – Left: Fourier spectra of all sensors and arrays for the OGIM survey. Right: ambient vibration H/V ratio for all sensors and for all arrays.

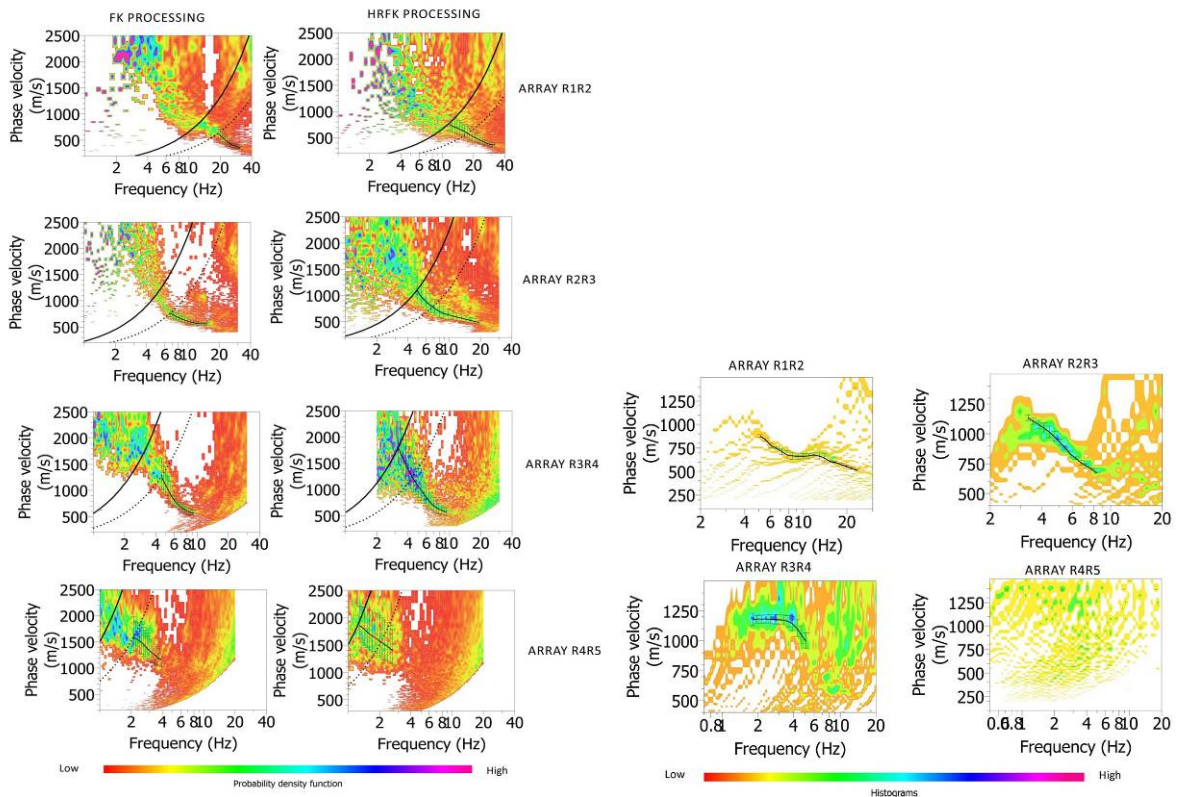


Figure 5 – Left: FK and HRFK processing and corresponding picked DCs for all arrays of the OGIM survey. Right: MSPAC processing and corresponding picked DCs for all arrays of the OGIM survey.

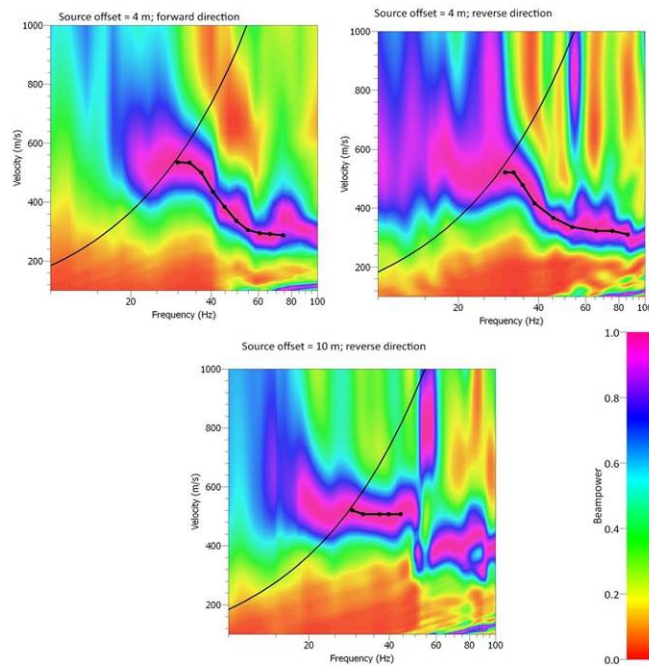


Figure 6 – MASW “beampower” processing and corresponding picked DCs for all horizontal (Love) polarization and shot locations.

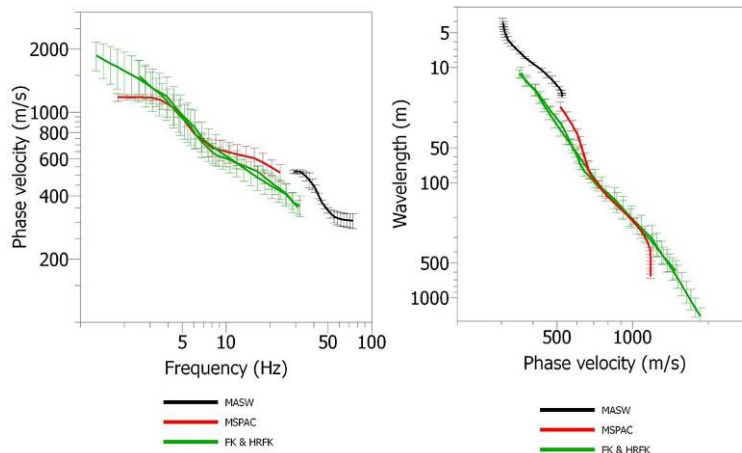


Figure 7 – Merge of all dispersion curves in both frequency-velocity plot (left) and wavelength-velocity plot (right).

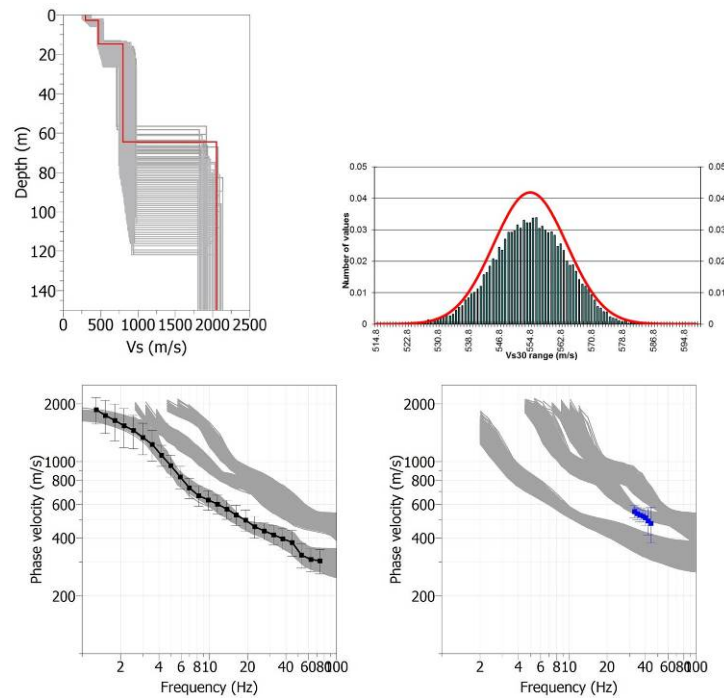


Figure 8 – Inversion results. Left: ensemble of statistically acceptable Vs profiles explaining the observed dispersion data within their uncertainty bounds. The red line shows the best misfit profile. Bottom: theoretical dispersion curves computed from the ensemble of inverted shear-wave velocity profile for Rayleigh phase (left) and Love phase (right). The dots indicate measured phase velocities +/- standard deviation.

5. Results – Soil class reattributions

At each station we developed a set of “acceptable” velocity profiles and the best estimated velocity profile. For few stations (especially in the Pyrenees where the acquisition did not benefit of the same redundancy of sensors and variety of array dimensions than in Alps), different hypothesis of mode attributions were addressed, leading to few sets of results. These results could then be derived in terms of Vs30 and EC8 soil classes. The Table 1 shows these results for the 28 stations for which the processing is now complete, associated to the geological condition of each station. Figures 9 show the obtained profiles. For two stations (both from Pyrenees, with the above mentioned limitations) the recorded data was not good enough to derive velocity profile at a significant depth.

In comparison with previous works on RAP station soil class estimation (this comparison could be done on 17 stations since they were studied by both works): 3 previously assumed “A class” stations are now downgraded to B class; 1 previously assumed “A class” station is now downgraded to C class; 1 previously assumed “B class” station is now downgraded to C class. No “upgraded” station was found. In terms of Vs30 values, 13 stations have now lower values than the previous estimation, 2 stations have now higher Vs30 value, 2 remain unchanged (within a +/- 10% range).

This overall observation shows that soil quality of network stations are usually overestimated when classification are not based on in situ measurements (this was already observed on other networks, like in Italy, see e.g. [5]).



Table 1 – Summary of the main results in terms of Vs30.

Station	Vs30 (m/s)	Geological conditions	Station	Vs30 (m/s)	Geological conditions
CALF	1806	Upper Jurassic (Oxfordian) karstified limestones.	OGDH	195	Post-Würmian alluvial and lacustrine deposits, overlying deep Jurassic limestones.
GRN	1042	Upper Jurassic limestone and marls alternations.	OGIM	623	Recent torrential cones / alluvial deposits, overlying deep Jurassic limestones and marls.
IRPV	662	Sand and molassic Miocene deposits overlying Oligocene marls.	OGLE	782	Fractured granites and schists.
IRVG	2020	Upper Jurassic (Tithonian) limestones.	OGMA	850	Würmian glacial deposits overlying Jurassic limestones and marls.
NALS	184	Quaternary alluvium deposits overlying deep Jurassic limestones.	OGME	390	Recent alluvial deposits overlying a terrace, overlying deep Cretaceous limestones.
NBOR	1331	Jurassic (Tithonian and Kimmeridgian) limestones.	OGMU	1106	Upper Jurassic limestone-marl alternations.
OCLD	380	Quaternary deposits overlying Oligocene and volcanic deposits.	OGPC	624	Recent alluvial and lacustrine deposits valley overlying deep Jurassic limestones.
OCOL	969	Hercynian granite.	PYAS	1003	Shallow quaternary deposits overlying Mesozoic limestones.
OCOR	1090	Quaternary colluvium overlying anatexites.	PYAT	1078	Lower Cretaceous (Albian) marls.
OGAN	1110	Cretaceous (Urgonian) limestone, weathered in surface.	PYBB	740	Cretaceous (Albian / Cenomanian) limestones and marls alternations.
OGAP	265	Würmian fluvio-glacial deposits overlying deep Cretaceous limestones.	PYLO	1501	Lower Cretaceous limestones.
OGBL	200	Recent alluvial and lacustrine deposits overlying Cretaceous limestones.	PYLU	383	Quaternary alluvial deposits overlying Devonian mudstones.
OGCA	1332	Cretaceous (Valanginian) limestone.	PYOR	310	Quaternary deposits (or weathered formations) overlying magmatic rocks (migmatites).
OGCH	1415	Upper Jurassic limestones.	SURF	522	Morainic Würmian deposits overlying Albian-Cenomanian flyschs and black shales.

6. Implication: is there any reference station?

8 sites out of the 22 investigated sites presented here (PYAS, PYLI, PYLL, PYLO, OGAN, OGCH, OGLE, and OGMU) were previously considered by Drouet et al. (2010) ([3]) as reference stations within a generalized inversion work. Within this work, these stations were assumed to have a Vs30 value of 2000 m/s. All Vs30 values determined within the framework of the present work are much lower.

Beyond the discussion about the Vs30 values, an important issue is the notion of “reference station”. If we focused on PYAS and PYLI, even if these two sites belong clearly to the EC8 “A” soil class, they both show a thin layer of low-velocity material with a thickness of few meters (due to a weather zone or thin quaternary colluvium deposits). This leads to a very high frequency site effect. The Figure 10 illustrates this feature showing the 1D transfer functions computed with “best estimated” and the one thousand profile sets for both PYAS and PYLI sites. The “A class” information is definitely not sufficient to characterize accelerometric site.

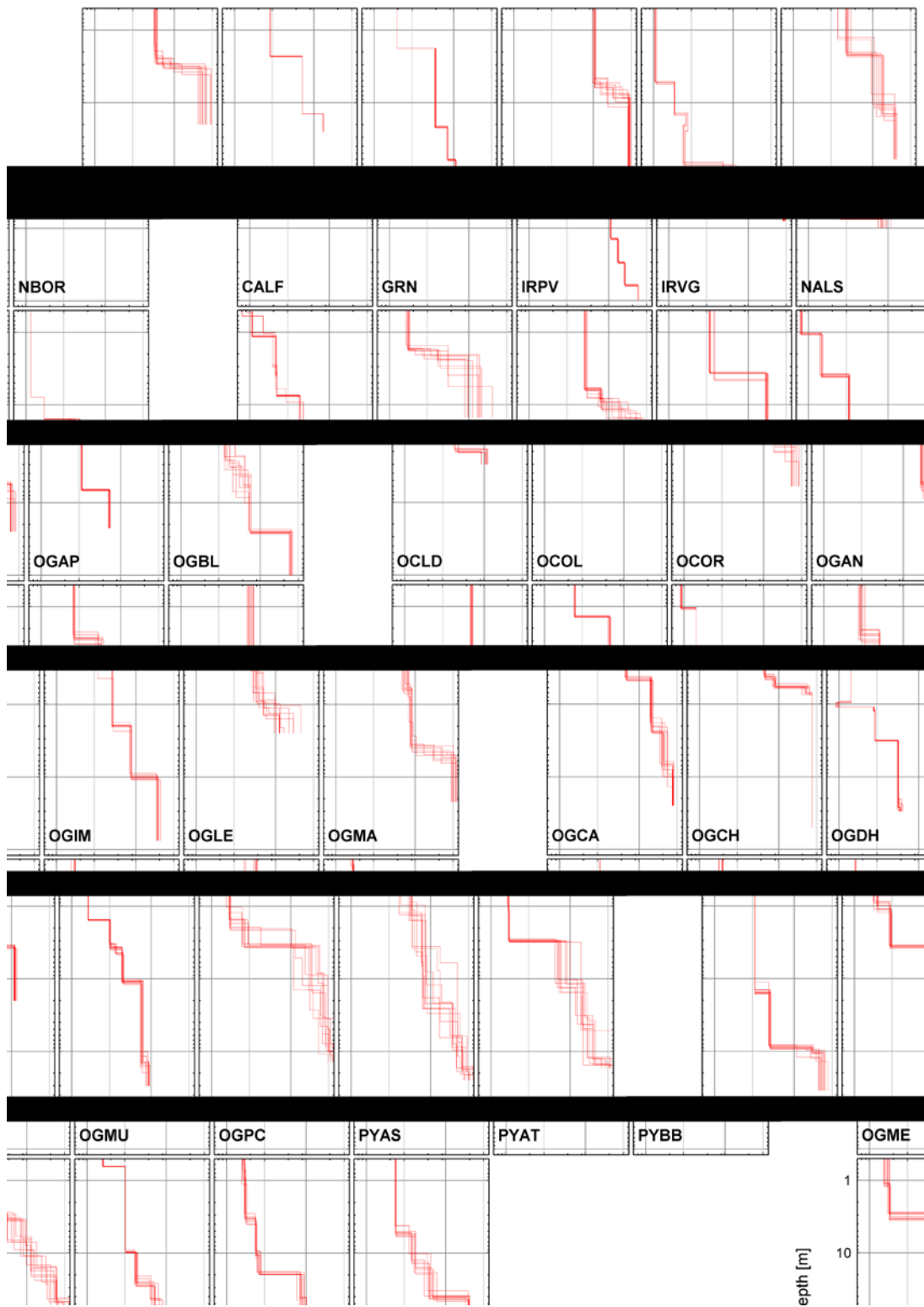


Figure 9 – ‘Acceptable’ V_s profiles obtained by inversion for the 28 sites that led to successful processing. For each site, a set of 10 profiles randomly chosen within the full set of ‘acceptable’ profiles are shown.

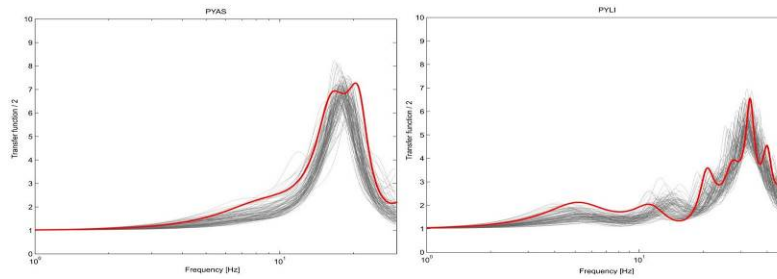


Figure 10 – 1D transfer functions computed with “best estimated” Vs30 profile (red) and the one thousand profile sets deriving from the “acceptable misfit” approach (gray) for both PYAS and PYLI sites.

7. Importance of recording Love waves and using it within inversion process

In most common surveys, only Rayleigh waves are recorded and considered for inversion. In our survey, we recorded both Rayleigh waves (with vertical geophones and excitation) and Love waves (with horizontal geophones and excitation) for MASW acquisition and we both processed them. For AVA data, we recorded the wave-fields with 3 component seismometers that could also allow Love and Rayleigh processing (even if we only processed them yet with vertical component, and hence, for Rayleigh wave dispersion curve determination).

In several cases, and especially on rock sites, the Love wave MASW acquisition allowed us getting a better dispersion curve than the Rayleigh wave MASW acquisition. The figure 11 gives an example of such case for the OGCA station. On the Rayleigh acquisition, the “beam power” image is very complicated and it is difficult, if not impossible, to “pick” a relevant DC curve. On the contrary, on the Love acquisition, it is easy to pick a consistent DC (even if the beam power image is not perfect).

On the inversion process itself, the fact of being able to proceed to a joint inversion of Rayleigh and Love wave allows to obtain a better constrained inversion and a more reliable velocity profile set. The figure 12 shows the example of the OGCA site. On this figure, the “measured DC curves” (in black with errors bars) are presented with the theoretical DC curves (fundamental and higher modes) deduced from the velocity profile set obtained by inversion. On this site, the Love acquisition allows to better constrain the velocity model within the first meters below surface, and especially the weathered zone thickness and associated Vs velocity. This information is important to understand the high frequency content of accelerograms recorded at such stations.

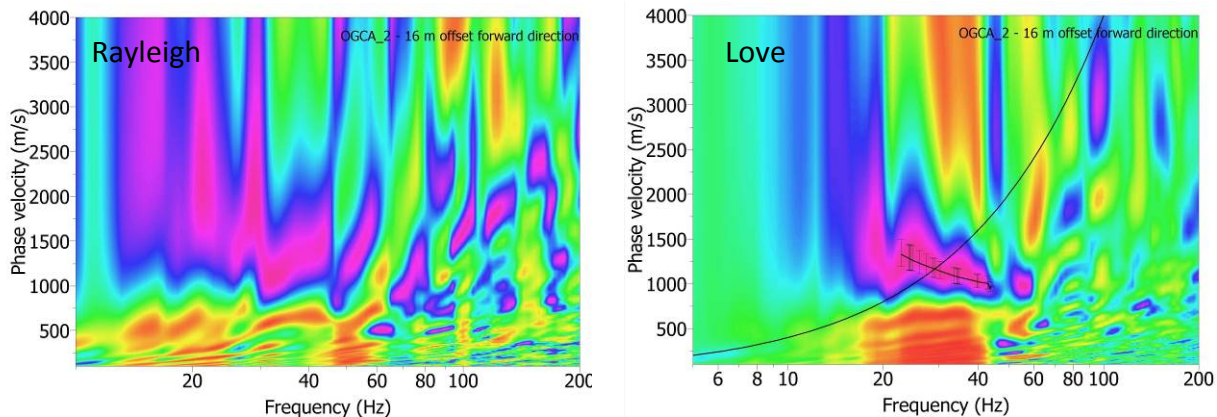


Figure 11 – Rayleigh (left) and Love (right) MASW beam power image at the OGCA site. Love acquisition produces here a more “readable” image that allows the DC curve to be picked.

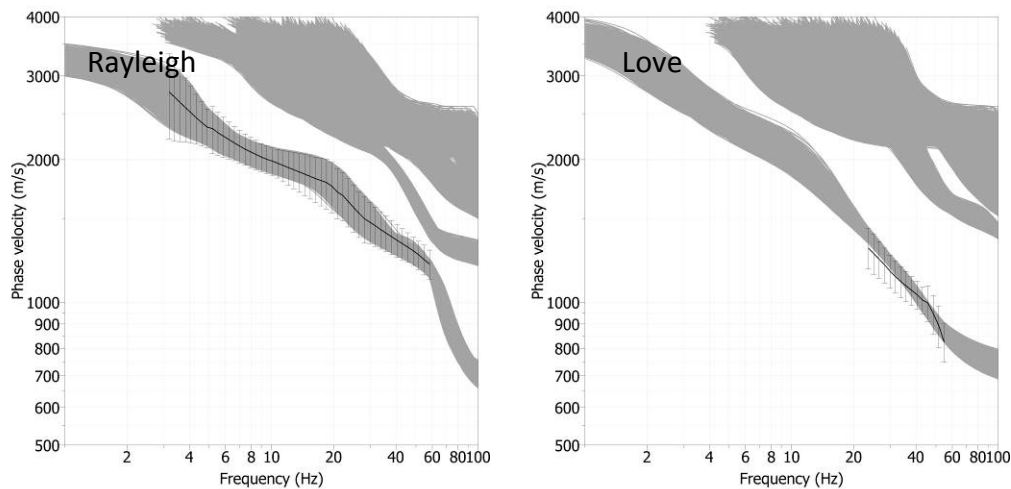


Figure 12 – Theoretical dispersion curves computed from the ensemble of inverted shear-wave velocity profiles obtained by inversion. The black dots indicate measured phase velocities (Rayleigh wave phase at left and Love wave phase at right).

8. Methodological feedback and conclusions

Even if logistical context is sometimes difficult, using surface-wave based methods are suitable for accelerometric station characterization, even on rock sites (where the applicability of these methods was sometimes disputed).

It was usually possible to achieve a complete survey for one station in one working day, with 5 to 6 motivated operators when the weather was OK... Conversely, the processing is time consuming (one working week for one geophysicist) and the inversion procedure have to be supervise by an expert in surface wave methods.

We recommend the use of a rather high number of sensors for AVA (15 sensors in our study) with the proposed double-circle geometry. The difference within the result quality between the Pyrenees stations (where we was not able to use double-circle geometry) and Alps is high. We also strongly recommend the joint use of active (MASW) and passive (AVA) methods in order to get “broadband” dispersion curves. The use of Love wave (for MASW in our case) is also very valuable in the inversion process in order to reduce the risk of misattribution of surface wave modes.

9. Acknowledgments

This work was conducted within the framework of the CASHIMA (funded by CEA, ILL and ITER Organization) and SIGMA (funded by EdF, CEA, Areva and Enel) research programs.

We would like to thank all the contributors of this work (especially for help on the field) who are not in the author list due to lack of place: Alice RENAULT (Soldata), Anne LOEVENBRUCK (CEA/LDG), Anthony BONJOUR (BRGM), Aurore LAURENDEAU (CEA/LDG), Catherine PEQUEGNAT (ISTERre), Cécile CRETIN (ISTERre), Cédric GUYONNET BENAIZE (CEA/CAD), Claire LABONNE (CEA/LDG), Clément DESBORDES (CEA/CAD), Corine LACAVE (Résonance), David WOLYNIÉC (ISTERre), Déborah SICILIA (EdF), Didier BRUNEL (GeoAzur), Diego MERCERAT (CEREMA), Emeline MAUFROY (ISTERre), Emmanuel CHALJUB (ISTERre), Etienne BERTRAND (CEREMA), Florence RENALIER (Soldata), Franck GRIMAUD (OMP), Franck TILLOLOY (BRGM), Isabelle DOUSTE-BACQUE (ISTERre), Isabelle DOUSTE-BACQUE (ISTERre), Jean LETORT (ISTERre), Jean-Pierre DESLANDES (ISTERre), Julie REGNIER (CEREMA), Laetitia FOUNDOTOS (CEA/CAD), Marc WATHELET (ISTERre), Mathieu CAUSSE (ISTERre), Michel PERNOUD (CEREMA), Mickaël LANGLAIS (ISTERre), Paul CALOU (CEA/LDG), Philippe



GUEGUEN (ISTerre), Pierre-Yves BARD (ISTerre), Robin BARBIER (BRGM), Roser HOSTE-COLOMBER (CEA/LDG), Sadrac SAINT FLEUR (GeoAzur), Stéphane NETCHSCHEIN (IRSN), Sylvette THOMASSIN (Résonance), Vincent BOUTIN (CEA/LDG), Vincent PERRON (CEA/CAD).

10. Copyrights

16WCEE-IAEE 2016 reserves the copyright for the published proceedings. Authors will have the right to use content of the published paper in part or in full for their own work. Authors who use previously published data and illustrations must acknowledge the source in the figure captions.

11. References

- [1] Garofalo F., S. Foti, F. Hollender, P.Y. Bard, C. Cornou, B.R. Cox, M. Ohrnberger, D. Sicilia, M. Asten, G. Di Giulio, T. Forbriger, B. Guillier, K. Hayashi, A. Martin, S. Matsushima, D. Mercerat, V. Poggi, H. Yamanaka, 2016, InterPACIFIC project: Comparison of invasive and non-invasive methods for seismic site characterization. Part I: Intra-comparison of surface wave methods, *Soil Dynamics and Earthquake Engineering*, 82, 222-240.
- [2] Garofalo F., S. Foti, F. Hollender, P.Y. Bard, C. Cornou, B.R. Cox, A. Dechamp, M. Ohrnberger, V. Perron, D. Sicilia, D. Teague, C. Vergniault; 2016, InterPACIFIC project: Comparison of invasive and non-invasive methods for seismic site characterization. Part II: Inter-comparison between surface-wave and borehole methods, *Soil Dynamics and Earthquake Engineering*, 82, 241-254.
- [3] Drouet S., Cotton F. and Gueguen Ph., V_s30 , κ , regional attenuation and M_w from accelerograms: application to magnitude 3–5 French earthquakes, 2010, *Geophysical journal international*, doi: 10.1111/j.1365-246X.2010.04626.x.
- [4] Wathelet, M., 2008, An improved neighborhood algorithm: parameter conditions and dynamic scaling, 2008, *Geophysical Research Letters*, 35. Vamvatsikos D, Cornell CA (2002): Incremental dynamic analysis. *Earthquake Engineering & Structural Dynamics*, **31** (3), 491-514.
- [5] Pileggi D., Rossi D., Lunedei E. and Albarello D., Seismic characterization of rigid sites in the ITACA database by ambient vibration monitoring and geological surveys, 2011, *Bull Earthquake Eng* (2011) 9:1839–1854.